

# Experimental report

22/02/2024

**Proposal:** 5-41-1128

**Council:** 10/2020

**Title:** Investigating High-Tc Spiral Order in YBaCuFeO<sub>5</sub> Multiferroic Single Crystal

**Research area:** Materials

**This proposal is a new proposal**

**Main proposer:** Jose Luis GARCIA MUNOZ

**Experimental team:** Oscar Ramon FABELLO ROSA

**Local contacts:** Oscar Ramon FABELLO ROSA  
Jose Alberto RODRIGUEZ VELAMAZAN

**Samples:** YBaCuFeO<sub>5</sub> single-crystal

Instrument	Requested days	Allocated days	From	To
D10	12	0		
D3 CPA	4	4	27/05/2021	31/05/2021

## Abstract:

The low-magnetic ordering temperatures critically restrict the potential uses of magnetoelectric multiferroics. YBaCuFeO<sub>5</sub> displays magnetism-driven ferroelectricity at unexpectedly high temperatures. This structure being one of the best candidates [Nature Comm 7, 13758 (2016), Science Adv. 4(10), eaau6386 (2018)] to switchable, magnetism-driven ferroelectricity at zero field. This system shows an extraordinary tunability of its spiral ordering temperature, which can be extended beyond ambient temperature by manipulating the Cu/Fe chemical disorder.

However, both a sinusoidal and a spiral magnetic order can give account of the magnetic intensities of the incommensurate phase from neutron powder diffraction patterns. Although the spiral solution is usually adopted to explain ferroelectricity in polycrystalline samples, there is no yet magnetic refinements of this phase using full single-crystal data. This experiment is aimed to definitively remove the ambiguity between the sinusoidal and spiral models in the incommensurate phase of a quality YBaCuFeO<sub>5</sub> crystal. To our knowledge, our sample presents the highest TS reported for YBCFO crystals.

# Experimental Report (D10: 5-41-1153) (D3: 5-41-1128)

## D10- Measurements. Zero Field (ZF) study. prop. 5-41-1153

The proposal 5-41-1153 contained two parts using D10. **First**, the study of the nuclear and magnetic structures in Zero Field (ZF). **Second**, a study under external magnetic field ( $H < 5$  T) on D10 in the two-axis mode using the 6T cryomagnet. We had time to do the first part (Zero Field study) but not the second part (study of the magnetic field induced transitions that we identified from magnetometry measurements along particular directions).

Single crystal neutron diffraction data was collected on a crystal with  $T_S = 195$  K (the highest reported in a YBCFO crystal), on the four-circle diffractometer D10, using  $\lambda = 2.36$  Å. Main nuclear and magnetic data collection was done at  $T = 10$  and 200 K. The program RACER was used to integrate the  $\omega$ - and  $\omega$ - $2\theta$ -scans and to correct them for the Lorentz factor. Structural and magnetic refinements were carried out using FullProf. Extinction corrections were applied following the model of Becker-Coppens.

The atomic positions were refined using the  $P4mm$  symmetry, and the Cu/Fe occupancies in the two pyramids of the unit cell were known from previous D9 measurements on the same crystal. At the spiral transition the collinear magnetic phase with  $\mathbf{k}_1 = (1/2 \ 1/2 \ 1/2)$  transforms under cooling into the spin modulated  $\mathbf{k}_2 = (1/2 \ 1/2 \ 1/2 \pm q)$  phase **Fig. 1(A)**. The evolution of the magnetic modulation  $q_S(T)$  in the crystal is shown in **Fig. 1(B)**.

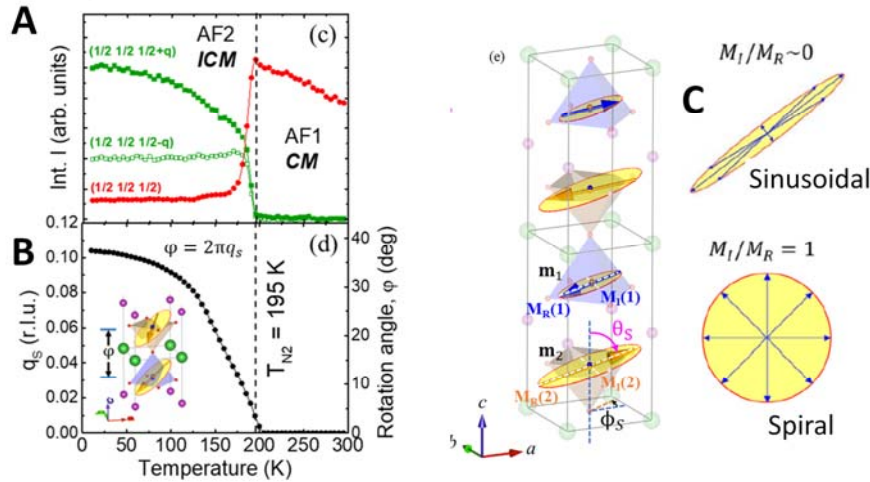


**Figure 1.** (A) Temperature dependence of the neutron integrated intensities of CM  $(1/2 \ 1/2 \ 1/2)$  [ $\mathbf{k}_1$ ] and ICM  $(1/2 \ 1/2 \ 1/2 \pm q)$  [ $\mathbf{k}_2$ ] magnetic reflections. (B) Evolution with temperature of the discommensuration  $q_S$  of the spiral phase. The twist angle  $\phi$  (canting) formed by the two spins of a bipyramid in the spiral phase is also shown ( $\phi = 2\pi q_S$ ). (C) Opposite limits (models) of the eccentricity (sinusoidal modulated versus spiral).

## D3- Measurements. prop. 5-41-1128:

D3 was used for spherical neutron polarimetry (SNP) measurements using the CryoPAD equipment ( $\lambda = 0.832$  Å). Zero-field neutron polarimetry measurements were done at 200, 100 and 10 K. The efficiency of the polarization at all temperatures was corrected from several measurements of  $P_{zz}$  on the (111) nuclear reflection. We used the Mag2Pol program for analyzing and fitting the spherical neutron polarimetry data.

**AF1 collinear phase.** The commensurate magnetic order (AF1) was satisfactorily refined from the integrated magnetic intensities associated to  $\mathbf{k}_1$  (Fig. 2(A)). The refinement to the spherical neutron polarimetry data of the commensurate AF1 phase was fully consistent with D10 data, including the fraction of coexisting collinear AF1 domains (Fig. 2(B)).

We fully determined the collinear magnetic order, the magnetic easy axis and anisotropy, and the respective fractions of the two twin magnetic domains. A full description of the refined magnetic order in the collinear magnetic domains can be found in the submitted manuscript (Ref. 1).

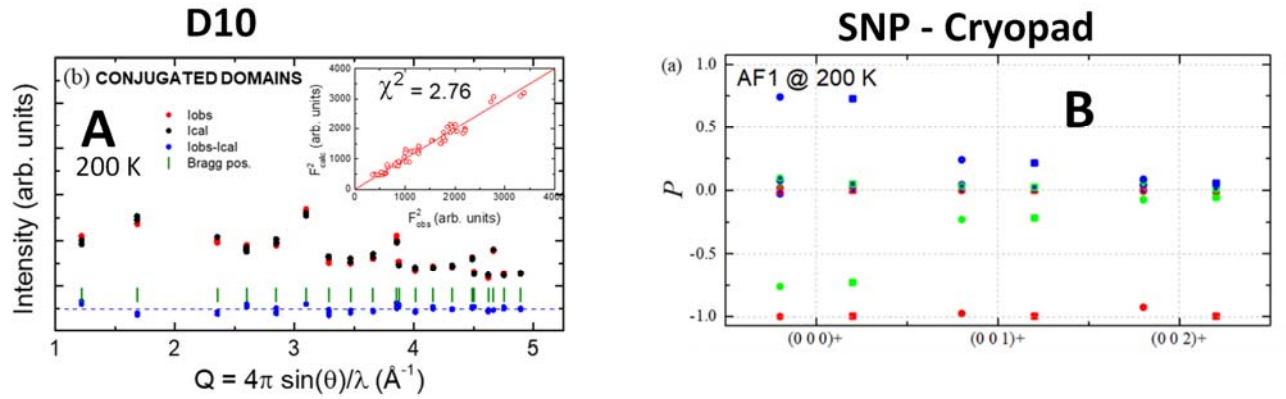


**Figure 2. AF1 phase:** (A) Final magnetic refinement of the collinear AF1 phase at 200 K [ $\mathbf{k}_1=(1/2,1/2,1/2)$ ] (D10 data). (B) D3 (SNP): observed (circles) and calculated (squares) polarization values  $P_{if}$  for the three directions  $x$  (red),  $y$  (green), and  $z$  (blue) in the local coordination system.

**AF2 incommensurate phase (Zero field).** The details of the incommensurate magnetic ordering were thoroughly investigated by unpolarized (D10) and polarized (D3) single crystal neutron diffraction at 10 K (Fig. 3), overcoming the critical limitations of neutron powder diffraction.

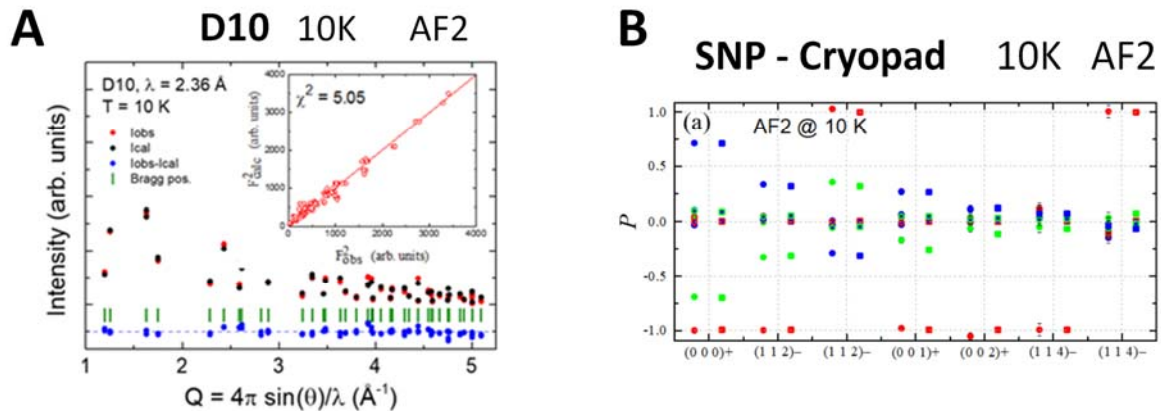


**Figure 3. AF2 phase (ZF):** (A) Best neutron refinement at 10 K (D10@ILL) of the incommensurate integrated magnetic intensities for the AF2 magnetic phase. (B) D3 (SNP): Refinement to the spherical neutron polarimetry data for the incommensurate AF2 phase at 10K (D3@ILL).

**Spherical neutron polarimetry.** The validity and robustness of the circular spiral model (Fig. 1(C)) was further investigated using polarized neutrons. At D3 we could access magnetic reflections associated with the incommensurate propagation vector  $\mathbf{k}_2=(1/2, 1/2, 1/2\pm q)$ . The crystal was cooled down from the paramagnetic

state to 100 K and 10 K in E-field conditions (+8 kV along the z-direction). Up to 5 incommensurate reflections were investigated with polarized neutrons. The polarization elements ( $P_{ij}$ ) measured at 10 K are shown in **Fig. 3(B)**, which also shows the refinement to the SNP data including the appropriate types of magnetic domains.

Independent but consistent results were obtained by fitting of unpolarized SCND (four-circle diffractometer D10) and Spherical Neutron Polarimetry (D3) data (**Fig. 3**). Different types of magnetic domains were considered depending on the distinct models investigated. The emerging magnetic model corresponding to best fits is not described in this report. It has been described and discussed in Ref. 1, which is based on the present experiment and the combination of D10 and D3 results.

The magnetoelectric response was explored at 100 K by means of an electrical field E applied parallel to z, namely along the (1 -1 0) axis of the crystal. The crystal was cooled down from the paramagnetic state to 100 K under an E-field of +18.2 kV/cm. We studied the changes in the magnetic configuration and the proportion of the two chiral domains under application of the electrical field. The neutron polarization measurements were repeated switching the E-field from +18.2 kV/cm to 0 kV/cm and finally to approx. -14.8 kV/cm. The changes with the field of the neutron polarization (cross) terms for the (112)- $\mathbf{k}_2$  reflection are disclosed in Ref. 1, where the influence of E on the magnetic domain populations has been discussed to the light of the incommensurate magnetic model previously determined.

Summarizing, collinear modulated and non-collinear spiral models, including the analysis of magnetic conjugated and chiral domains, were confronted to neutron data collected for our YBCFO single-crystal ( $q_s = 0.104$  r.l.u.). This study has removed essential ambiguities persisting in the literature, still based on powder samples, covering the gap created by the lack of single-crystal investigations. The emerging magnetic models corresponding to best fits for AF1 and AF2 are not described in this report. They have been described and discussed in Ref. 1 (submitted manuscript), which is based on the present experiment using D10 and D3 results. A natural continuation requires to study the response of the spiral to external magnetic fields ( $H < 5$  T), which can be performed on D10 (in the two-axis mode) using the 6T cryomagnet. Our results concerning the magnetic anisotropy of the spiral in this crystal, obtained in this experiment, confirm the importance of study the magnetic field induced transitions that we have identified from M(H) measurements with  $H//a$ . Of the major importance is to assess the possible manipulation of the spiral orientation by relatively small applied magnetic fields in these novel high-temperature spiral multiferroic candidates (induced by disorder).

**Ref. 1.** A. Romaguera, O. Fabelo, N. Qureshi, J. A. Rodríguez-Velamazán and J.L. García-Muñoz, manuscript submitted (2024) to Nat. Commun. , based on this experiment. The results from D10 and D3 were complemented with additional neutron measurements previously collected on Cyclops and on the hot-neutrons four-circle diffractometer D9 ( $\lambda=0.837$  Å).